

[illegible]

Contents

Table of Contents	i
List of Figures	i
List of Tables	ii
0.0.1 SiV center in a Plasmonic Double Bowtie Antenna	1
Index	8

List of Figures

1	Localizing suitable nanodiamonds	2
2	Spectrum of a nanodiamond containing at least one SiV center	3
3	Confocal scan of a gold double bowtie antenna	4
4	4
5	(a) Measured PL spectrum of the emitter after placing the nanodiamond into the nanoantenna, (b) Convolution of the spectrum of the measured PL spectrum of the emitter before pick-and-place (see Figure ??) and the simulated resonance spectrum of the nanoantenna (see Figure ??).	5
6	(a) The $g^{(2)}$ function of the preselected nanodiamond hosting few nanodiamonds. A dip at $g^{(2)}(0)$ is present, however it does not decrease below 0.5. While this indicates that more than one SiV center is present, a small number of SiV centers cause a dip in the $g^{(2)}$ function instead of no dip at all which would be measured under coherent emission cps zu a.u. aendern	
	(b) Saturation curve of the same emitter zahlen fuer sat eintragen	
	. Data points are black, fitted curve red.	7
7	(a) Spectrum of the preselected nanodiamond hosting few SiV centers. (b) Measured spectrum after transfer of the preselected nanodiamond into the double bowtie antenna.	7
8	(a) Spectrum of the nanodiamond hosting few SiV centers coupled to the double bowtie antenna after the emitter bleached. (b) Background corrected spectrum of the transferred nanodiamond in the double bowtie antenna. Peaks are fitted, results of the fits are the colored lines. For background correction, the spectrum in (a) was used.	8

List of Tables

0.0.1 SiV center in a Plasmonic Double Bowtie Antenna

In the following we report on our attempts to couple SiV centers to gold double bowtie nanoantennas in order to study the properties of the resulting integrated system. Ideally, a suitable nanodiamond containing exactly one SiV center is placed in the center of the antenna. The term suitable is used to summarize both desirable spectroscopic properties such as narrow-bandwidth saturated single-photon emission as well as technical requirements such as nanodiamond size and degree of isolation on the surface. Naturally, the odds of identifying and addressing a nanodiamond fulfilling all these criteria simultaneously are small. As a result identifying a perfect candidate for coupling is prohibitively time-consuming.

To mitigate this difficulty we decided to relax the condition of exactly one SiV center per nanodiamond and initiate our explorative work with nanodiamonds containing several, potentially many active SiV centers. Relying on $g^{(2)}(0)$ measurements we identify two interesting classes of nanodiamonds. The first class consists of nanodiamonds containing large ensembles of SiV centers acting as coherent emitters. The fluorescence light received from large ensemble of emitters is mainly coherent, leading to a flat response in the $g^{(2)}(0)$ function. The second class of nanodiamonds we investigate features nanodiamonds hosting multiple SiV centers. As a result relevant $g^{(2)}(0)$ measurements report weak but discernable anti-bunching dips. Both classes have in common that relevant nanodiamond specimen are significantly easier to obtain than nanodiamonds containing singleton SiV centers. Thus nanodiamonds containing ensembles of SiV centers as well as nanodiamonds containing few SiV centers are both valid starting points for our work. It is likely that the experience gained during our preliminary explorations will be valuable once nanodiamonds containing singleton SiV centers become available.

In the following sections we report on our efforts to couple nanodiamonds containing SiV centers to antennas. We illustrate the coupling process and its challenges and discuss relevant results regarding the coupling of nanodiamonds of the classes described above. We close the chapter with a short discussion and suggestions for further research.

Nanodiamonds Containing Ensembles of SiV centers Coupled to Antennas

The nanodiamonds exploited for the approach of coupling multiple SiV centers to an antenna were produced by a wet-milling process from a CVD diamond film¹. The solution of nanodiamonds which exhibit a median size of 100 nm were spin-coated on an iridium substrate treated with Piranha etch. To ensure that a pre-characterized nanodiamond exhibiting preferred optical properties (eg. narrow linewidth, high count rate) is later found again, the iridium substrate was engraved with reference cross markers produced by a focused ion beam prior to the spin-coating process. After spin-coating, the sample was placed in an oven for 3 hours at 450 °C to oxidize the surface and remove any residual graphite and amorphous carbon.

To determine the position of nanodiamonds on the original substrate, first a scan with a commercial laser scanning microscope (LSM) was performed as described in ?? . Figure 1a shows a part of an obtained LSM image. The cross marker can easily be identified, the

¹wet-milling performed by A. Muzha, group of A. Krueger, Julius-Maximilians Universität Würzburg, diamond film grown by group of O. Williams, School of Engineering, Cardiff University

black dots are nanodiamonds. After transferring the sample into the confocal setup, confocal fluorescence light scans of the corresponding areas are performed to identify nanodiamonds containing active emitters. The scanned area is shown in Figure 1b. It corresponds to the area shaded blue in Figure 1a. Thus, upon close inspection some of the bright spots appearing in the fluorescence light scan can be associated with selected nanodiamonds in Figure 1a by eye. The correspondence between the SEM and LSM images in conjunction with the cross-markers on the substrates allows to precisely locate preselected nanodiamonds containing suitable emitter in the SEM.

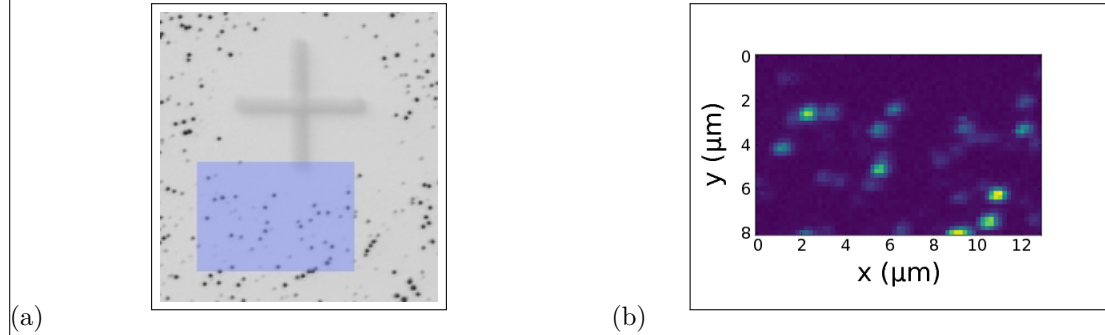


Figure 1: (a) Picture recorded with a commercial high resolution laser scanning microscope. Black dots are individual nanodiamonds. The cross-marker serves as an orientation aid. The area shaded in blue represents the photoluminescence scan in image (b). (b) Photoluminescence scan of a $8\mu\text{m} \times 13\mu\text{m}$.

Figure ?? shows the spectrum stemming from one such preselected nanodiamond. The ZPL peak exhibits a wavelength of $(738.55 \pm 0.01)\text{nm}$ and a linewidth of $(5.00 \pm 0.03)\text{nm}$. These numbers correspond well to the ZPL of unstrained SiV centers and therefore allows us to deduce that the studied nanodiamond contains at least one SiV center. Photon autocorrelation measurements revealed that the nanodiamond contains multiple SiV centers.

The picking part of the pick-and-place process was analogous to the procedure used for moving VCSELs described in ??. Notably, the gold surface of the plasmonic antenna exhibited strong adhesion forces between the antenna surface and the nanodiamond. Once the nanodiamond touched the gold, it could not be picked up again with the tungsten tip. The nanodiamond first touched the antenna structure a few nanometers away from the gap and immediately stuck to the surface, on top of one of the triangles. Therefore, the nanodiamond had to be pushed into the gap with the nanomanipulator tip. This process caused some damage to the antenna structure. The damage is visible as black area at the tip of the top triangle in ??. However, FDTD simulations of damaged antennas reveal that this modification of the antenna hardly influences the antenna resonance.

Remark:

Die figure die den damage zeigen soll fehlt komplett. Vielleicht sollte man die zusammenpacken mit der FDTD simulation, die zeigt, dass das nix ausmacht.

After successful placement, the antenna sample is installed in the confocal setup. The structure where the nanodiamond was placed is searched observing the sample surface in a CCD image under white light illumination. Representative resulting images are shown in ??. A scan of the antenna is performed in the confocal setup using a 660 nm continuous wave laser.

bild dazu

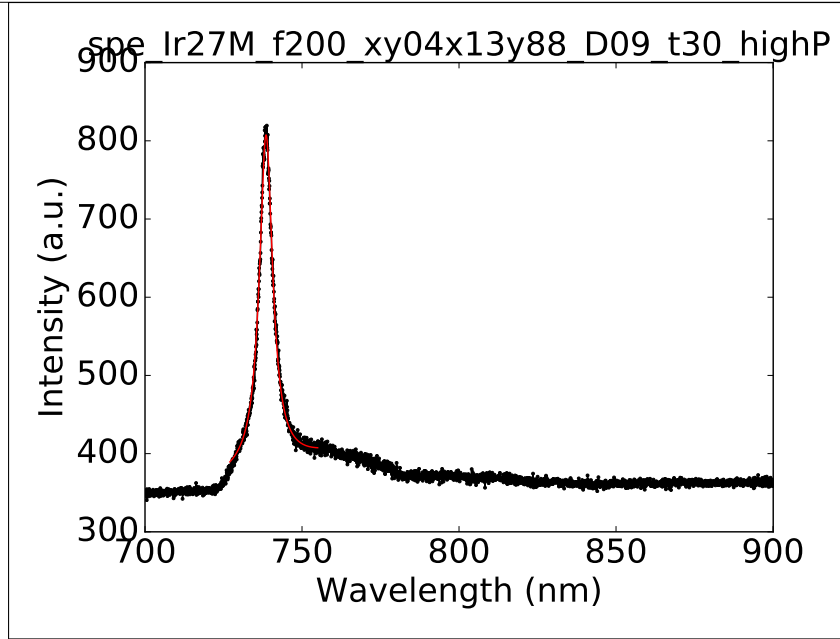


Figure 2: PL spectrum of the emitter in the preselected nanodiamond at room temperature. Black: experimental results; red: fit to experimental data, which yields a ZPL center wavelength of (738.55 ± 0.01) nm and a linewidth of (5.00 ± 0.03) nm. The narrow center wavelength and the almost invisible sideband makes this nanodiamond an excellent candidate for coupling to an antenna.

It serves to locate the middle of the antenna structure and therefore the nanodiamond which had been placed there. An outline of the rings is visible in an overview scan of the antenna structure shown in Figure 3a. Zooming in to the exact center of the rings, some of the edges of the bowtie antenna are vaguely visible in Figure 3b.

These images suffices to approach the nanodiamond close enough to measure a PL spectrum. The PL spectrum of the SiV center in the nanodiamond gives insight to the effect of the nanoantenna on its emission. The result is displayed in Figure 5a.

To rule out artifacts, a spectrum of an antenna of the same dimensions without nanodiamond is recorded (Figure 4). The additional peak at a lower wavelength is attributed to the antenna resonance mode.

To verify this, we convolute the experimental PL spectrum of the nanodiamond measured before placing it in the nanoantenna (Figure ??) with the intensity spectrum of the nanoantenna obtained by simulations (??). The resulting spectrum is given in Figure 5b, and is in good agreement with the measured spectrum in Figure 5a, confirming that indeed the extra peak is due to the antenna resonance.

Kopplung experimentell machbar. Kopplung erfolgreich - simulation in agreement with measurements. Enhancement nicht quantifizierbar weil ensemble of emitters.

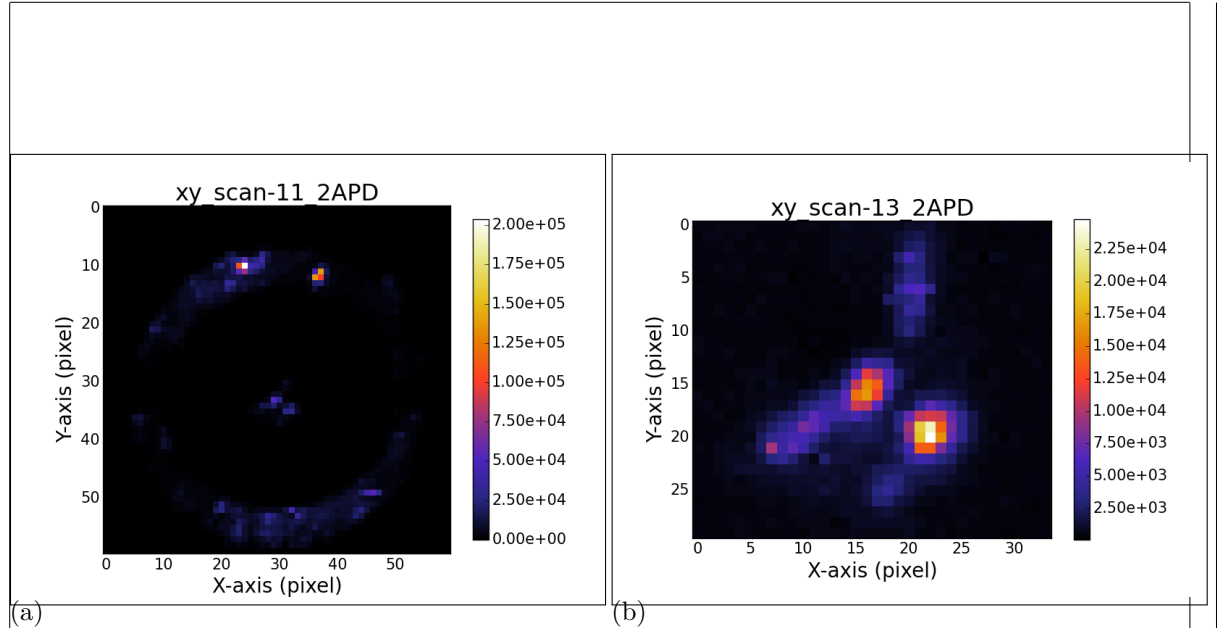


Figure 3: (a) Confocal scan of the double bowtie antenna where a nanodiamond containing multiple SiV centers had been placed. The rings are visible. (b) Detail scan of the triangles of the same antenna structure, which make up the double bowtie antenna. While the separate triangle cannot be seen, some edges and two bright spots are visible. To identify the place of the nanodiamond we compare the middle point of the rings in (a), the point of intersection of the edges and the bright spot and conclude that the upper bright spot in (b) is the location of the nanodiamond.

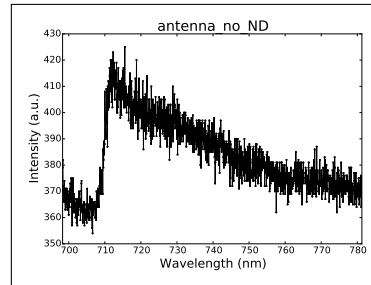


Figure 4

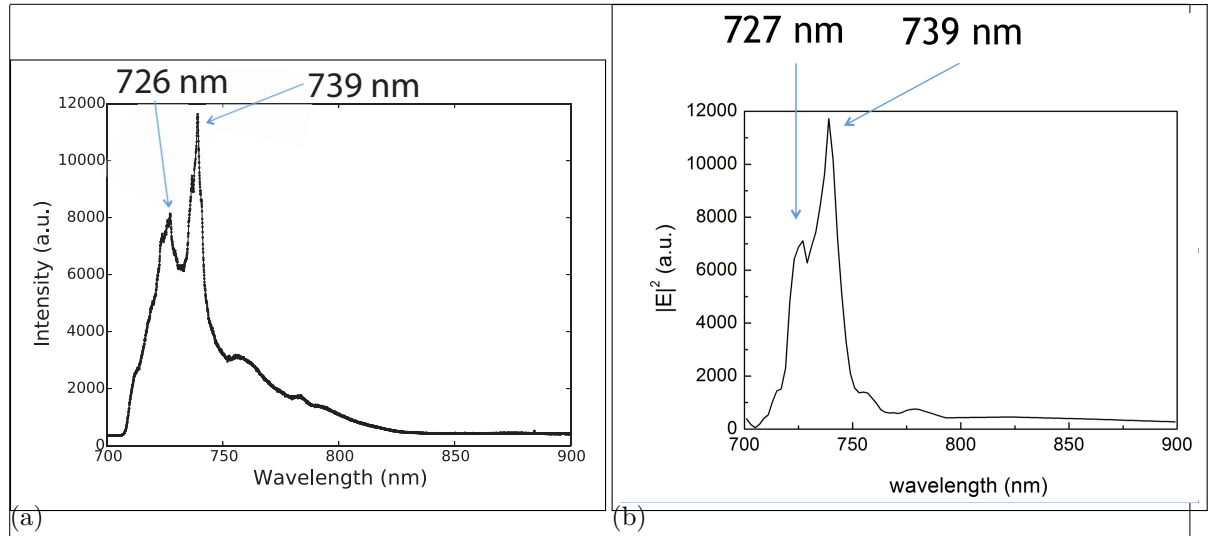


Figure 5: (a) Measured PL spectrum of the emitter after placing the nanodiamond into the nanoantenna, (b) Convolution of the spectrum of the measured PL spectrum of the emitter before pick-and-place (see Figure ??) and the simulated resonance spectrum of the nanoantenna (see Figure ??).

Nanodiamond With Few SiV center Coupled to Antenna

As the experiment of coupling a nanodiamond with an ensemble of SiV centers proved to be very successful, the next step was to select a nanodiamond with only few SiV centers, i.e. that it exhibits countrate saturation and a dip in the $g^{(2)}$ function. In this section, coupling a nanodiamond containing only few SiV centers to a double bowtie antenna is reported. It is an intermediate step between coupling The origin sample used for this experiment is an iridium substrate onto which a solution of nanodiamonds were drop-casted. Starting material for the nanodiamonds was a electronic grade diamond film produced by the company rho-BeSt coating (now CarbonCompetence). It was then milled in a bead-assisted sonic disintegration process² to nanodiamonds of a size of . The nanodiamonds were drop-casted at 60 °C onto an iridium substrate containing cross markers which had been treated with Piranha etch.

Preselecting a nanodiamond with a single SiV center is imposes additional constrains to the suitability of an nanodiamond if compared to a nanodiamond with multiple SiV centers. First, only a small percentage of the technically suited nanodiamonds (size, isolation) contain a single SiV center, second, damage due to electon radiation during pick-and-place. The position of the SiV centers on the substrate surface was performed in the same way as described in ??. The identification whether bright spots in the scan were suitable emitter was performed as follows: First a saturation curve was recorded. Countrate saturation is only a necessary and not a sufficient measure for single photon emission, hence the saturation measurement alone does not prove that the emitter in question is single. However, it takes only a few seconds to record a saturation measurement compared to potentially hour-long measurements of $g^{(2)}$ functions. Therefore, it is a quick selection method to evaluate potential candidates. Once an emitter with a saturating countrate was found, a spectrum was recorded to prove that the emitter in question is indeed an SiV center. At last, the $g^{(2)}$ function was recorded. We

²A. Krueger, Julius-Maximilians Universität Würzburg

checken,
ob
angaben
passen

groesse
einfuegen

successfully found an SiV center with a small dip in the $g^{(2)}$ function. While the dip is too small to account for a single SiV center, it indicates the presence of only few SiV centers. Hence, we proceeded by transferring the host nanodiamond to the antenna structure. The SiV center coupled to the antenna structure was then spectroscopically investigated in the confocal setup. First, we recorded a spectrum (spectrum A). The result of the first recorded spectrum revealed a multitude of peaks. To ensure that the peaks are no artifacts due to deficient alignment, we rechecked the alignment which proved to be precise. We initiated another measurement of the spectrum. However, this time the recorded spectrum only showed a broad background (spectrum B). After checking in the confocal scan that the measurement was performed at the correct position, we had to conclude that the emitter bleached shortly after recording spectrum A.

As mentioned earlier, the electron radiation may damage SiV centers in nanodiamonds. The electron radiation might have put the SiV center into an unstable state. Although we were still able to measure one spectrum, further application of energy from the laser seems to have permanently bleached the SiV center. While we cannot solidify this conclusion with further experimental evidence, we observed in earlier independent measurements that some SiV centers bleach after electron radiation and that some SiV centers bleach after an extended laser irradiation [1]. The observations in this measurement suggest a combination of the two effects.

We performed FDTD calculations of the selected SiV center in the host nanodiamond in the plasmonic double bowtie antenna as described in the previous section. We used spectrum B to for background correction of spectrum A and fitted the measured peaks (Figure 8b). In the simulations, we do not see the peaks between 700 nm to 750 nm that we recorded in the measurement. Hence, we conclude, that not additionally to the observed photobleaching, also the emitter's spectrum was modified in the pick-and-place process. While it is not possible to pinpoint exactly which circumstance caused the modification, possible candidates are.

To gain further insight, we performed FDTD calculations with antenna damage and different dipole orientation. To be able to include the dipole orientation into the calculations, a dipole emitter with a broad emission instead of a narrow emission peak has to be used. Therefore, the convolution method as described in the previous section is more adequate for our purpose, as the SiV center exhibits a very narrow emission peak. However, these calculations give further insight. First, the antenna damage does not have a big effect on the spectra, however the dipole orientation changes the results drastically (??). Therefore, future experiments should include polarization measurements to experimentally quantify the impact of the emitter orientation.

Outlook: Coupling a Nanodiamond With a Single SiV center to the Plasmonic Double Bowtie Antenna

To effectively state the emission enhancement of the SiV center by the plasmonic double bowtie antenna, a single SiV center is necessary. A correct measure for the emission enhancement is the saturation count rate. The saturation count rate is proportional to the inverse of the emitter's lifetime. Hence, if there are two or more emitters present, photons of the individual emitters are emitted randomly, which renders a correct saturation measurement impossible. However, finding SiV centers in nanodiamonds which fulfill both spectroscopic ($g^{(2)}(0) \approx 0$, saturation, narrow ZPL spectrum) and technical (size, isolation of nanodiamonds) constraints turned out to be a very time-consuming work.

We investigated different kinds of nanodiamonds in the search of nanodiamonds exhibiting

put in pictures

enter candidates and explain why

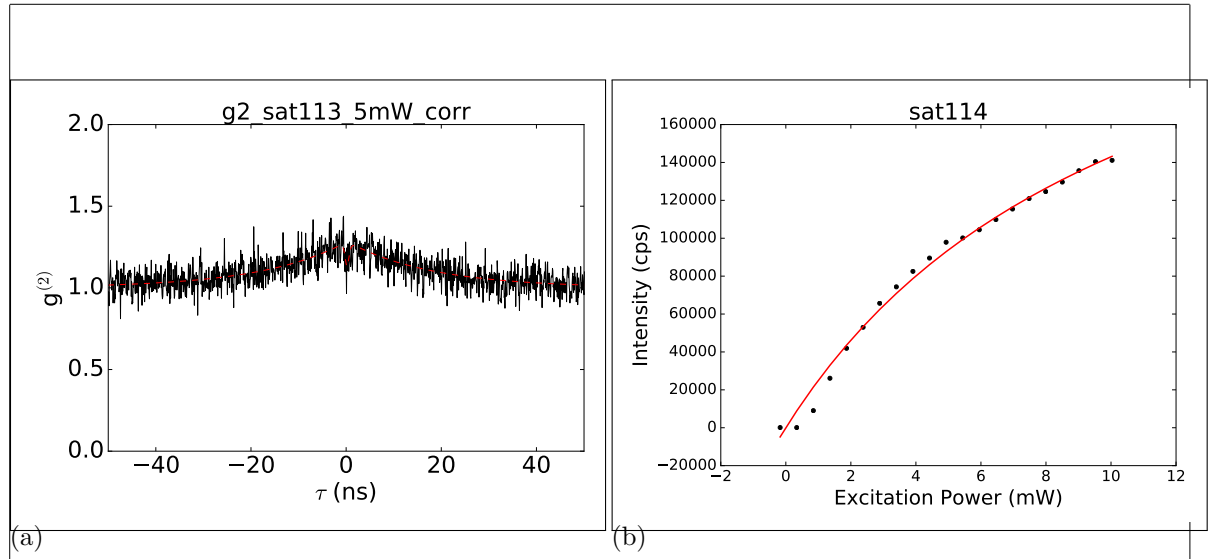


Figure 6: (a) The $g^{(2)}$ function of the preselected nanodiamond hosting few nanodiamonds. A dip at $g^{(2)}(0)$ is present, however it does not decrease below 0.5. While this indicates that more than one SiV center is present, a small number of SiV centers cause a dip in the $g^{(2)}$ function instead of no dip at all which would be measured under coherent emission

cps zu a.u. ändern

. (b) Saturation curve of the same emitter

zahlen fuer sat eintragen

. Data points are black, fitted curve red.

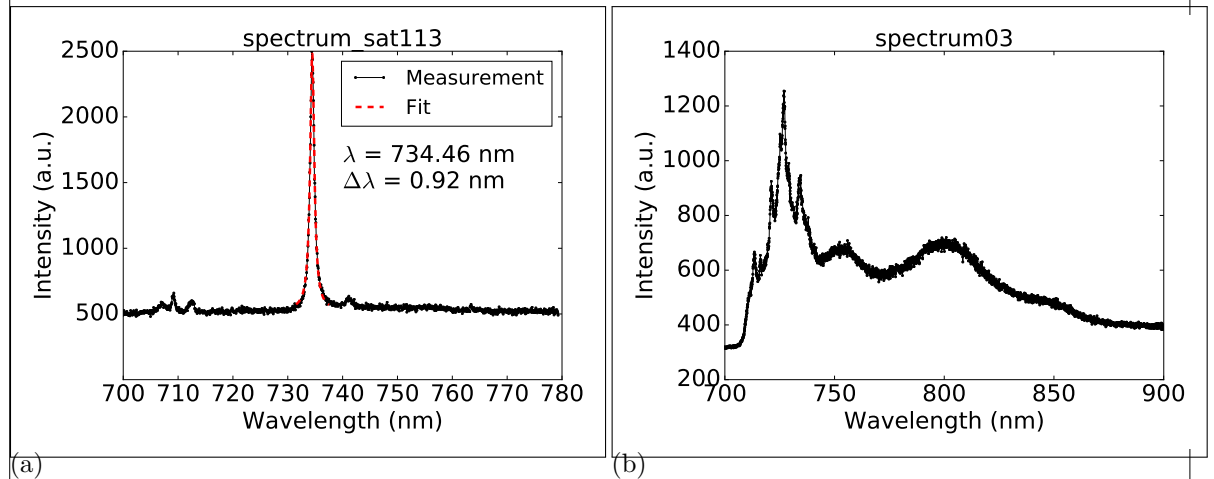


Figure 7: (a) Spectrum of the preselected nanodiamond hosting few SiV centers. (b) Measured spectrum after transfer of the preselected nanodiamond into the double bowtie antenna.

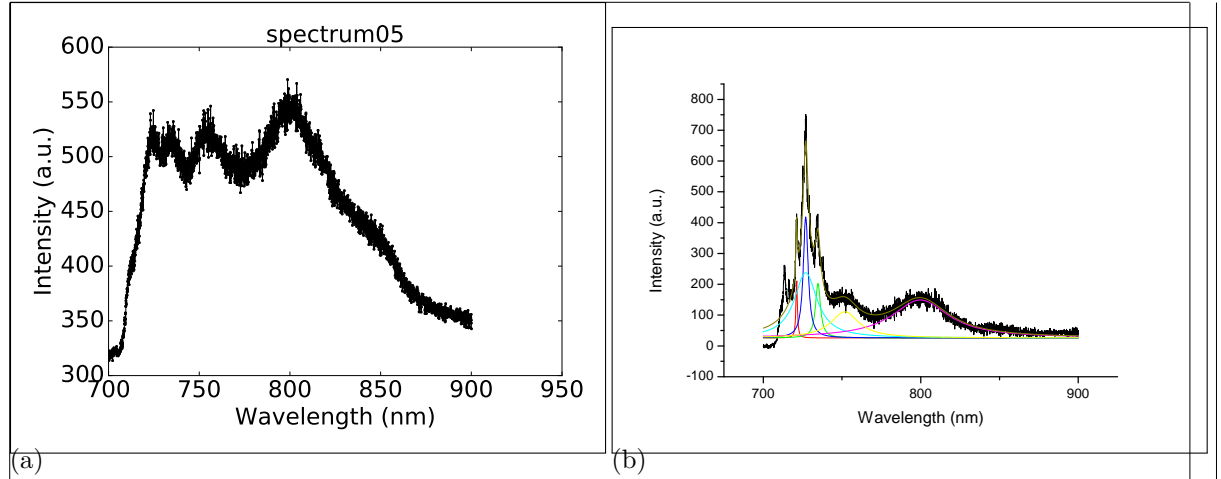


Figure 8: (a) Spectrum of the nanodiamond hosting few SiV centers coupled to the double bowtie antenna after the emitter bleached. (b) Background corrected spectrum of the transferred nanodiamond in the double bowtie antenna. Peaks are fitted, results of the fits are the colored lines. For background correction, the spectrum in (a) was used.

optimal spectroscopic and technical parameters. We were able to fulfill the size requirements posed by the pick-and-place process and antenna design by producing different patches of different sizes of nanodiamonds and took the ones which were best suited. We also developed a good isolation of the nanodiamonds on the substrate by treating the iridium substrate with Piranha etch and tuning the amount of diamond solution drop-casted onto the substrate. This leaves us with the need of a higher probability of exactly one SiV center per nanodiamond. Parameters which have an impact on the quantity of SiV centers per nanodiamond are the initial SiV center density in the starting material and the nanodiamond size. Once the time constraint of finding a single SiV center in a nanodiamond is overcome, we can apply the extensive methods and knowledge gained by the reported procedures to couple a single SiV center to a plasmonic bowtie antenna.

To our knowledge, our experiments were the first time an SiV center in a nanodiamond was coupled to a plasmonic bowtie antenna. The extraordinarily precise correlation of the theoretically predicted and the experimentally recorded spectrum of an ensemble of SiV centers in a nanodiamond make this process a promising candidate for future applications.